EVS30 Symposium
Stuttgart, Germany, October 9 - 11, 2017

Proof of concept of a method for on the fly cycling behavior analysis and its use for reducing range anxiety

Auguste Colle[1], Rien Leenders[2], Emilia Motoasca, Bram Rotthier, Jan Cappelle
KU Leuven Technology Campus Ghent, Gebroeders De Smetstraat 1, 9000 Ghent, Belgium
[1]*auguste.colle@kuleuven.be,* [2]*rien.leenders@kuleuven.be*

Abstract

Cycling range prediction is, more often than not, completely absent in commercially available Electrically Power Assisted Cycles (EPACs); most EPAC users are satisfied with a simple battery status indication. However, the rising use of EPACS with an assistance speed up to 45 $\mathrm{km/h}$, the so-called speed pedelecs, increases energy consumption drastically in such a way that further lead to the reinstatement of range anxiety despite an unchanged trajectory. This paper introduces a range prediction algorithm by on-board collecting of GPS data and weather data and real-time analysis of the cycling style. By adding to this monitoring of battery power, a method to estimate the model parameters (drag area, rolling friction and cyclist power) is proposed and validated.

Keywords: bicycle, data acquisition, GPS, range, prediction

1 Introduction

New European type-approval legislation for L-category vehicles became effective on the first of January 2016, classifying speed pedelecs as L1e-B vehicles. The legal status of the speed pedelec in local traffic regulations differs from member state to member state. The impact of the different regulatory frameworks on the speed pedelec market remains to be seen. Although the speed pedelec market evolution in Belgium since the start of the mandatory registration from October 1st 2016 remains uncertain, already 2041 speed pedelecs were registered during the first three months [1].

A method to estimate the Remaining Cycling Range (RCR) for EPAC users is presented, specifically targeting the speed pedelec subgroup. These vehicles have reinstated the range anxiety that used to be a problem for the 25 $\mathrm{km/h}$ e-bikes [4]. However, the required power to reach 25 $\mathrm{km/h}$ on a light two-wheeler in flat and windless conditions, is ∼170 W. Cruising at a speed of 45 $\mathrm{km/h}$ in the same circumstances requires ∼815 W [2]. The battery capacity of speed pedelecs is rarely exceeding 500 Wh (the largest battery capacity found on the Flemish market was 1 kWh). With a measured energy consumption between 10 and 20 $\mathrm{Wh/km}$ on flat Flemish roads and a test group of Flemish speed pedelec cyclists that showed an average commuting distance of 26.9 km ending up with an empty battery is more realistic than one would think at first sight [3].

2 Physical model and parameter estimation

The EPAC's cyclist's and motor power expenditure (P_c and P_m respectively) is the sum of the power consumed due to aerodynamic drag P_a, rolling friction P_r, acceleration P_{ke} and change in height P_{pe}. This is mathematically formulated in Eq. (1) and further expanded in Eq. (2) into the respectively underlying physical quantities, yielding a set of 10 parameters/variables $\{P_c, P_m, \rho, C_d, A, v_g, v_a, C_r, m, s\}$.

$$P_c + P_m = P_a + P_r + P_{ke} + P_{pe} \tag{1}$$

$$
\begin{cases}
P_a = \dfrac{\rho \cdot C_d \cdot A}{2} \cdot v_g \cdot v_a^2 \\
P_r = C_r \cdot v_g \cdot m \cdot g \\
P_{ke} = m \cdot a_g \cdot v_g \\
P_{pe} = m \cdot g \cdot v_g \cdot s
\end{cases} \tag{2}
$$

The parameters mentioned can be divided into three categories:

- parameters related to the trajectory: $\{\rho, v_a, v_g, C_r, s\}$
- parameters related to the cyclist: $\{C_dA, m, P_c\}$
- unknown parameters that can only be estimated from on-board measurements

2.1 Trajectory related parameters

Variables related to the trajectory are: air density ρ $[\mathrm{kg/m^3}]$, projected wind speed v_a $[\mathrm{m/s}]$, ground speed v_g $[\mathrm{m/s}]$, rolling friction coefficient C_r [-] and slope s [-]. The set of variables $\{\rho, v_a, v_g, s\}$ is derived by the development of a web browser application based on Mapbox and Google Maps API [5],[6]. The web app runs on the cyclist's smartphone. In the web app, a user can route from one destination to another whereby latitude, longitude and height of the routing points are converted to continuous slope functions by means of a b-spline. Position changes are tracked by the smartphone's GPS as is the ground speed. Weather forecast is included by the use of Yahoo weather, giving current and future data on v_a, wind direction and temperature at the actual position of the cyclist [7]. Air density ρ is a function of height and temperature thus it can be calculated from previous data. Rolling friction coefficient C_r is unknown and will be estimated in section "Estimation of unknown model parameters".

2.2 Motor related parameters

Trying to measure the on road mechanical motor power in real-time is difficult. However, measuring the electric motor power in real-time may be relative simple and accurate. The mechanical motor power can be further inferred from a motor model that uses as input the measured electric motor power. As with most e-bikes [8], a Brushless DC (BLDC) motor is used for the test bicycle. A hub installation is chosen for the ease of deriving rotational motor speed. To estimate mechanical motor power (P_m), the parameters of an equivalent BLDC motor model are derived as explained in [9]. Given the battery power (P_{bat}) and the ground speed of the cyclist (v_g), the mechanical motor power (P_m) is calculated in accordance to Eq. (3), where R_a is the armature resistance, V_b is the voltage drop across the inverter, $R_{m\_ev} /\!/ R_{l\_v}$ are eddy current losses and mechanical viscous losses, $I_{m\_hf} + I_{l\_f}$ are losses due to hysteresis and mechanical friction.

$$
\begin{aligned}
P_m = P_{bat} - \Bigg[& R_a \cdot I^2 + \frac{(k_e \cdot \omega_m)^2}{(R_{m\_ev} /\!/ R_{l\_v})} \\
& + k_e \cdot \omega_m \cdot (I_{m\_hf} + I_{l\_f}) + V_b \cdot I \Bigg]
\end{aligned} \tag{3}
$$

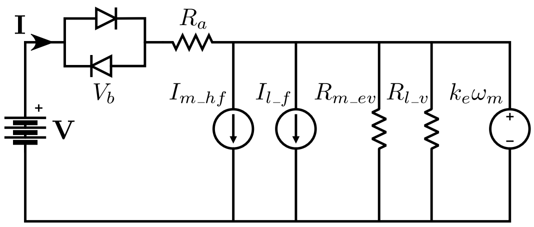

Figure 1: Equivalent circuit of BLDC motor

Table 1: Calculated model parameters

V_b $[V]$	R_a $[\Omega]$	$R_{m\_ev} /\!/ R_{l\_v}$ $[\Omega]$	$I_{m\_hf} + I_{l\_f}$ $[\mathrm{A}]$	k_e $[\frac{\mathrm{V \cdot s}}{\mathrm{rad}}]$
4.44	0.27	62.34	0.43	0.68

The model parameters, derived from locked-rotor and no-load tests, are given in Table 1. Results are shown in Fig. 2-5.

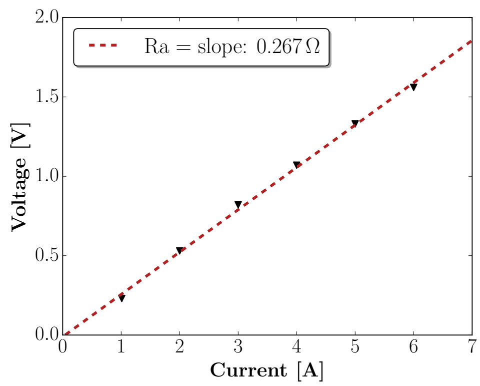

Figure 2: Locked-rotor test to determine R_a

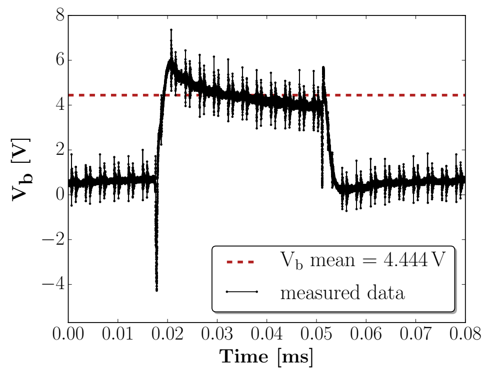

Figure 3: Rotor with load test to determine V_b

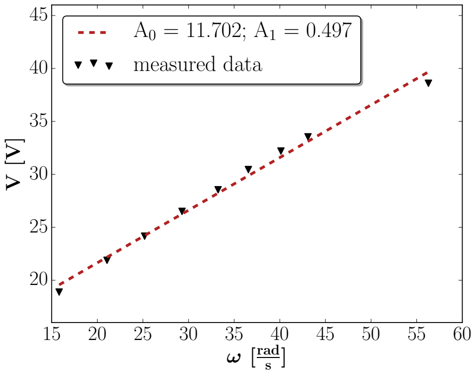

Figure 4: No-load test to determine k_e

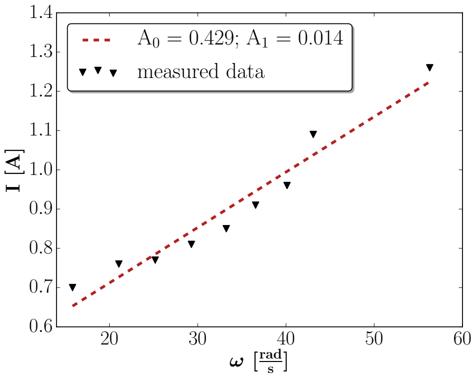

Figure 5: No-load test to determine $(R_{m\_ev}//R_{l\_v})$ and $(I_{m\_hf} + I_{l\_f})$

2.3 Cyclist related parameters

Variables related to the cyclist are combined drag area of the bike and cyclist C_dA $\left[\mathrm{m}^2\right]$, mass m [kg] and cyclist's power P_c [W]. The cyclist's mass m is a known parameter and can be manually entered in the web app. Ground speed v_g depends on the cyclist's behavior and is measured by the GPS of the cyclist's smartphone, see Sec. 2.2. Figure 6 presents the ground speed distribution during 13 days of commuting for one of the test persons of the KU Leuven speed pedelec test population. The cyclist's power P_c and drag area C_dA of the bike and cyclist are unknown and will be estimated in section "Estimation of unknown model parameters".

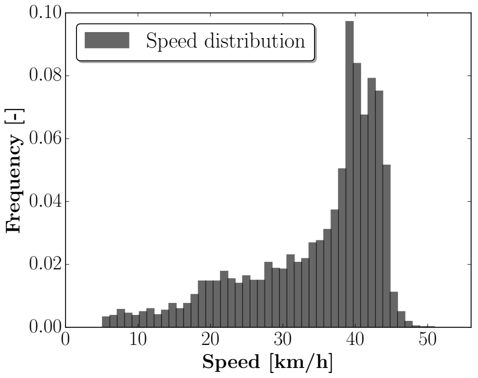

Figure 6: v_g distribution of a speed pedelec commuter

2.4 Estimation of unknown model parameters

Unknown model parameters are $\{C_r, C_dA, P_c\}$. They vary by cyclist, bicycle, cyclist's clothing, cyclist's position on the bicycle, tire pressure etc.[10] However, some assumptions on these parameters can be postulated and expressed in a probability distribution or prior. As such, the probability of finding a value for the rolling friction and drag area is assumed to be uniform and bound and are estimated to be in the ranges $C_r \in [0.002, 0.030]$ and $C_dA \in [0.2, 0.8]$. Mechanical losses are directly proportional to the ground speed and will result in an augmented rolling friction coefficient since they are not modeled separately. Which is why the upper bound on C_r is higher than what can be assumed when only regarding losses due to rolling. The cyclist's power is assumed to follow a Weibull distribution as shown in Fig. 9. For untrained cyclists, daily commuters and trained cyclists, one unit power is estimated to be P_c =80 W, 130 W and 180 W, respectively. The cyclist profile can be set in the web app.

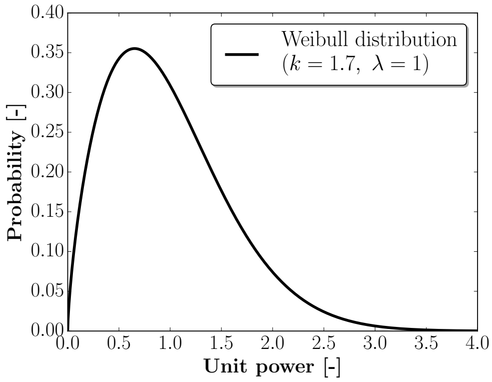

Figure 7: Prior on the cyclist's power P_c

Estimating the unknown parameters with their respective priors (p) is done by maximizing the likelihood of a set values for $\{C_r, C_dA, P_c\}$ given the estimated motor power $\hat{P}_{motor}$ and the measured motor power P_{motor} as given in Eq. (4).

Minimizing the negative of the log-likelihood function yields the same result as maximizing the likelihood function but simplifies calculation complexity. The result of this operation is shown in Eq. (5). The Nelder-Mead method is used for minimizing this function. Only time frames where velocity remains more or less constant (for that particular time frame) are taken into account yielding better estimates by eliminating the acceleration component in the estimation of motor power.

$$\hat{P}_{motor} = P_a + P_r + \cancel{P_{ke}} + P_{pe} - P_c$$
$$P_{motor} = P_{bat} - \left[R_a \cdot I^2 + V_b \cdot I + \frac{(k_e \cdot \omega_m)^2}{(R_{m\_ev}//R_{l\_v})} + k_e \cdot \omega_m \cdot (I_{m\_hf} + I_{l\_f}) \right] \tag{4}$$

$$L(P_{motor}, \hat{P}_{motor}) = -\ln \left[\frac{1}{\sqrt{2\pi\sigma^2}} \cdot e^{\left(\frac{-(P_{motor}-\hat{P}_{motor})^2}{2\sigma^2}\right)} \cdot p(\hat{C}_r, \hat{C}_{dA}, \hat{P}_c) \right] \quad (5)$$

3 Experimental set-up

The proposed model parameter estimation technique requires the installation of a small box (~8x5x7 cm^3) onto the speed pedelec containing a computer, the Raspberry Pi zero (RPi), on a custom made PCB which includes provisions to measure motor power (by means of communication with the speed pedelec's hardware or by direct measurement of current by means of a shunt resistor and voltage by means of a voltage divider). The RPi is configured as a web server providing access to all computed data. A smartphone is required to interface with the server and providing the server with trajectory related information (location, speed, weather, etc.). An overview of the system is given in Fig. 8.

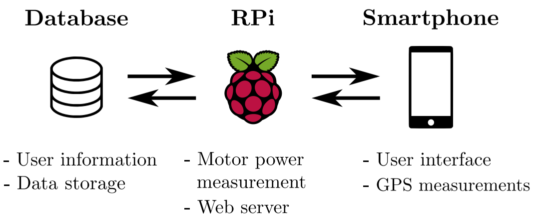

Figure 8: Schematic overview of set-up

To increase flexibility of motor control, a Cycle Analyst (CA) is installed [11]. The CA allows to, among others, regulate electrical assistance, limit electrical power, cycle at constant speed and use the bicycle as a scooter by means of a throttle. Configuration of the CA is done by adjustable presets based on which the CA dictates the behavior of the motor controller.

4 Results

4.1 $\mathbf{C_d A}$ and $\mathbf{C_r}$ estimation when $\mathbf{P_c = 0}$

The values of C_dA and C_r were, in a first attempt to validate the model, estimated by eliminating the cyclist's power from the optimization allowing easily reproducible experiments. The data was retrieved by cycling on a towpath without much interference from trees or houses, since these influence the wind speed. The CA was configured for constant speed, regulated by the throttle input. Two different positions were tested, cycling for about 20 minutes each in upright and hunched over position as shown in Fig. 9. Since the cyclist is prohibited to contribute to the power balance, the first experiment happened without pedaling.

Figure 9: Upright position ($C_dA = 0.53$) vs. hunched over position ($C_dA = 0.34$)

Unaffected by removing the bounding condition on C_r and C_dA or by different initial guesses, the optimization converges to the same solutions for each of both cycling positions, see Table 2. The results are well within expectation. Measured data and fit of a ride are shown in Figs. 10 and 11. The x-axis shows the measurement number and 1 unit roughly corresponds to 1 second (whenever new GPS information is available, a data point is logged. The frequency depends on, among others, the amount of satellites in range). The apparent delay between measured motor power and estimated motor power is due to the delay in the GPS measurements.

Table 2: Solution of optimization

	C_dA	C_r	P_c
Upright	0.53	0.02	0.00
Hunched over	0.34	0.01	0.00

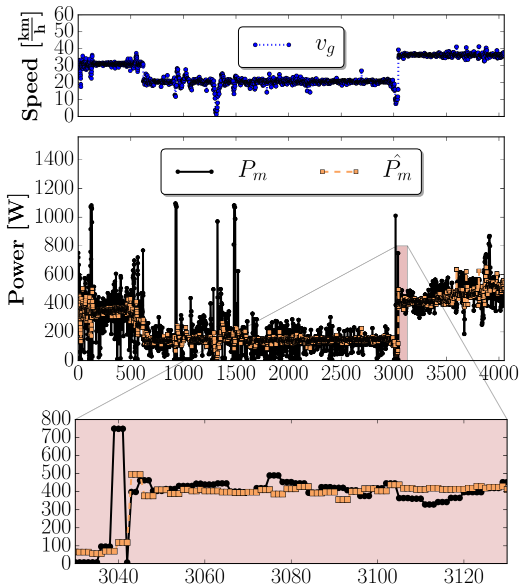

Figure 10: Data from upright position

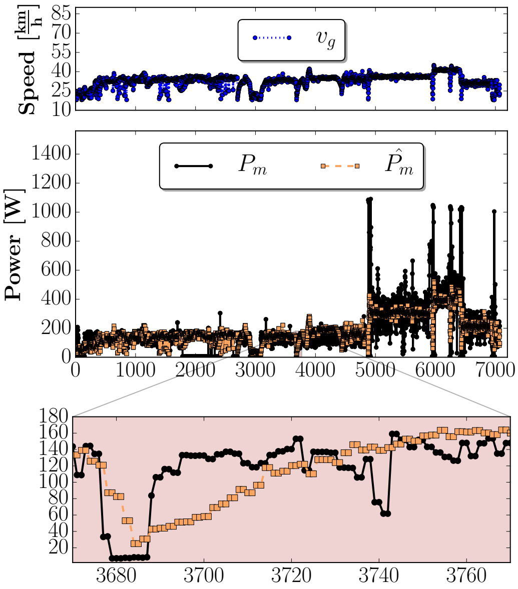

Figure 11: Data from hunched over position

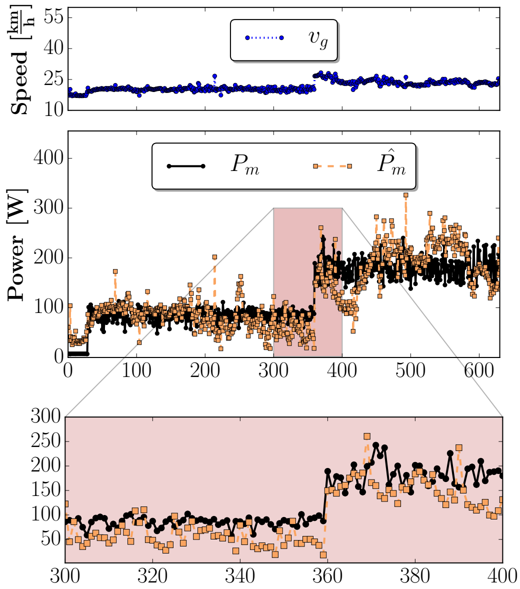

Figure 12: Data from upright position, boundaries on C_dA narrowed down to $[0.50, 0.60]$

4.2 $\mathrm{C_dA}$, $\mathrm{C_r}$ and $\mathrm{P_c}$ estimation on short trajectories

Estimating the three parameters when cycling in upright position on short trajectories ($< 5\,\mathrm{km}$) proves to be unstable since different lower boundaries on C_dA lead to different solutions. Based on the previous results, the range on C_dA was narrowed down to $[0.50, 0.60]$ and this yields the results in Table 3. Strong gusts of wind were experienced during cycling (there was an average predicted headwind of $38\,\mathrm{km/h}$) which are not modeled since the wind speed and heading are assumed to be constant and are retrieved from the nearest weather station (the weather data is updated on a 5 minute interval). This can explain why the minimization converges to a minimum for C_dA, lowering the impact of the gusts, at the expense of choosing a high value for P_c.

Table 3: Solution of optimization for a short trajectory, one unit power is assumed to be 130 W

	C_dA	C_r	P_c
Initial boundaries	0.2	0.03	1.57
Adjusted boundaries	0.52	0.01	1.31

Table 4: Solution of optimization of a long trajectory, one unit power is assumed to be 130 W

	C_dA	C_r	P_c
Adjusted boundaries	0.51	0.01	1.23

4.3 $\mathrm{C_dA}$, $\mathrm{C_r}$ and $\mathrm{P_c}$ estimation on long trajectories

In the expectation that the influence of gusts of wind should be mitigated when cycling for a longer period of time, data was collected from a 67 km ride, see Fig. 13. However, strong winds (average head wind of $41\,\mathrm{km/h}$) and the high density of buildings in Flanders do not provide for ideal test conditions. Plenty of gusts where experienced and the expected averaging of these gusts is unobservable. Results with the narrowed boundaries of $[0.50, 0.60]$ on C_dA are given in Table 4.

Figure 13: a 67 km ride from Ghent to Ostend

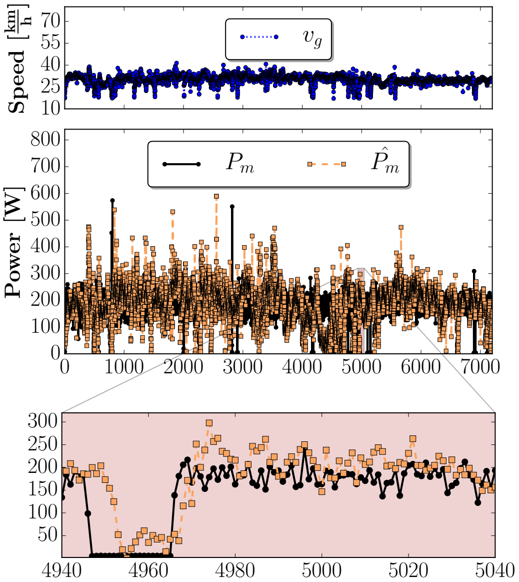

Figure 14: Data from upright position cycling from Ghent to Ostend, boundaries on C_dA narrowed down to $[0.50, 0.60]$

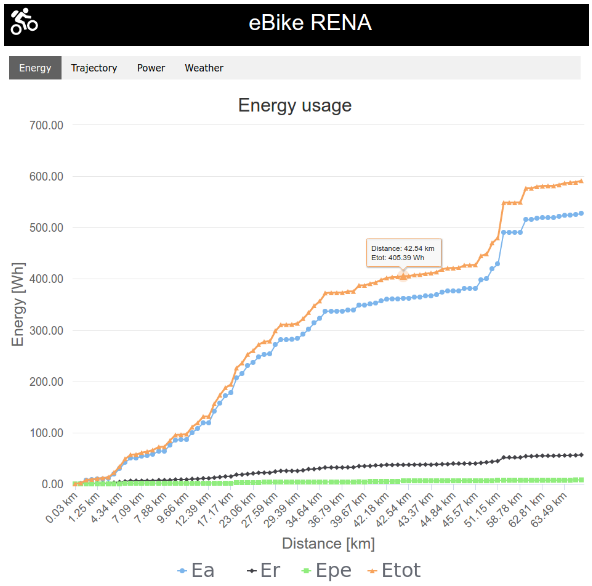

Figure 15: Expected energy expenditure when riding from Ghent to Ostend, screen shot of the energy tab in the web app

4.4 Range prediction and assistance control

Once C_r, C_dA and a measured probability distribution for P_c are derived from measurements, the total energy expenditure E_{tot} for cycling a trajectory can be estimated. This is implemented in the web app and shown in Fig. 15. The remaining battery energy E_{bat} is given by the state of charge of the battery which can be retrieved by simple coulomb integration or by communication with the on-board hardware of the speed pedelec. E_{bat} can be translated to remaining mechanical energy by multiplying it with the average modeled motor efficiency of the last n measurements. From this, the maximum allowable assistance factor AF_m can be calculated as shown in Eq. 6. Since the CA can be programmed on the fly by the RPi, the assistance factor can be dynamically adjusted to prioritize reaching the target's destination without loss of electrical support.

$$\mathrm{AF}_m = \frac{\frac{\sum_{i=1}^{n} \eta_i}{n} \cdot E_{bat}}{E_{tot} - \frac{\sum_{i=1}^{n} \eta_i}{n} \cdot E_{bat}} \tag{6}$$

5 Future research

The demonstrated results indicate high sensitivity on presumed constant weather conditions, specifically the presumed constant wind speed and wind heading. Further research will include filtering of gathered data for C_dA and C_r estimation based on optimal weather conditions, this is in best case windless conditions. Improvements might also be made by data treatment before the parameter estimation, removing the offset from GPS measurements as a start.

6 Conclusion

A method has been proposed for on the fly estimation of the drag coefficient, rolling coefficient and cyclist's power. The method is based on the comparison between measured motor output power and predicted motor output power. Preliminary results of the method on raw collected data from different testing conditions provide a prove of concept but indicate high sensitivity on the presumed weather conditions from weather forecast. Once unknown model parameters are estimated they are used for calculating the total needed energy for cycling a trajectory. Comparison of the chemical energy stored in the cyclist's battery with the total needed energy is used to estimate the maximum allowable assistance factor prioritizing reaching the target's destination without loss of electrical support.

References

[1] Federale Overheidsdienst Mobiliteit en Vervoer, *Aantal inschrijvingen speed pedelec vanaf 1 oktober 2016*

[2] Bram Rotthier e.a. *The rise of the speed pedelec, restrained by legislation?*, EVS30 October 2017, Stuttgart, Germany.

[3] Bram Rotthier e.a. *The speed pedelec: a game changer for commuting in Belgium?*, Workshop on electric bicycle commuting, June 2016, Ghent, Belgium.

[4] J. Cappelle, Ph. Lataire, G. Maggetto, and P. Van den Bossche, *Electrically Assisted Cycling around the World*, The 20th International Battery, Hybrid and Fuel Cell Electric Vehicle Symposium, November 2003. Long Beach, California.

[5] *Mapbox*, https://www.mapbox.com/

[6] *Google Maps API*, https://developers.google.com/maps/

[7] *Yahoo*, https://developer.yahoo.com/weather/

[8] Jan Cappelle, *Performance Analysis of Pedal Electric Cycles: An Objective and Subjective Approach.* (2008)

[9] Takeo Ishikawa, Takuma Tsuji, Seiji Hashimoto and Nobuyuki Kurita, *A Simple Equivalent Circuit for Efficiency Calculation of Brushless DC Motors*, Journal of International Conference on ELectical Machines and Systems Vol.3, No. 1, pp. 24 60, 2014

[10] David Gordon Wilson, Jim Papadopoulos, *BICYCLING SCIENCE Third edition*, MIT Press 2004

[11] *Cycle Analyst*, http://www.ebikes.ca/product-info/cycle-analyst-3.html

Authors

Auguste Colle graduated in 2013 as electro-technical engineer. He has been active in the research group E&A on a variety of different projects. At present, he is researching mid-range battery balancing and has relevant experience on battery SOC estimation.

Rien Leenders graduated in 2013 as electro-technical engineer. At KU Leuven University, he has over three years experience in the field of energy monitoring. He is active in data-measurement, data-registration, electronic development of smart metering devices and the rebuild of automatic and manual transmissions.

Emilia Motoasca obtained a PhD-degree in Electrical Engineering from Delft University of Technology in 2003. Between 2003 and 2013 she worked at the Eindhoven University of Technology, Faculty of Electrical Engineering, as post doc and later on as an assistant professor. In 2015 she joined the research group Energy and Automation at KU Leuven as assistant professor with research interests in design and modelling of electric motors and drives applied to robotics, e-mobility and industrial processes.

Bram Rotthier graduated in 2012 as electrotechnical engineer at the Catholic University College Ghent. His master's thesis, written at Tampere University of Technology in Finland, dealt with the dielectric properties of ceramic coatings. He is currently working as a researcher for the E&A research group in the domain of electric vehicles.

Jan Cappelle graduated in 1999 as electro-mechanical engineer at the KU Leuven University. In 2008 he obtained a PhD in Engineering Sciences at the Vrije Universiteit Brussel. His PhD thesis was an objective and subjective study of the performance of electric bicycles. As associate professor at KU Leuven in power systems, he runs a research group in the domain of standalone hybrid power systems.